ACS ES&T Water

Editors' Choice

pubs.acs.org/estwater

Article

Uptake Kinetics of CrAssphage, PMMoV, Human Adenovirus 40/41, Norovirus GII, Enterovirus, and SARS-CoV-2 on Electronegative Membrane Passive Samplers

Adnan Ege Sener,* Leo Heijnen, Miranda de Graaf, Jeroen Langeveld, and Gertjan Medema

Cite This: *ACS EST Water* 2026, 6, 903−912

Read Online

ACCESS | Metrics & More | Article Recommendations | Supporting Information

ABSTRACT: Wastewater surveillance (WWS) of viruses can aid public health officials in monitoring community infection dynamics and act as an early warning system for the introduction of viral infectious diseases. In recent years, agile, low-cost devices called passive samplers have proven to be indispensable for targeted wastewater surveillance. However, the viral uptake kinetics are unexplored for most viruses, limiting the understanding of optimal deployment times and the representativeness of this sampling method for assessing community viral shedding. This study investigates the uptake kinetics of CrAssphage, Pepper Mild Mottle Virus, Human Adenovirus 40/41, Human Norovirus genogroup II, Enterovirus, and SARS-CoV-2 on electronegative membrane passive samplers. Viral uptake was modeled by linear and pseudo-first-order uptake models for up to 48 h (adjusted R^2: 0.89−0.99), with minimal saturation for 48 h. Bench-scale experiments revealed enrichment of Human Adenoviruses 40/41 on membranes compared to all other viral targets for 24−48 h deployment ($p < 0.05$), while differences were less pronounced with shorter deployment durations. This work highlights virus-specific interactions with passive samplers and how deployment times can affect the relative concentrations of viruses detected. Understanding these kinetics is critical for selecting appropriate sampling strategies and normalization methodologies for WWS of viral infectious diseases.

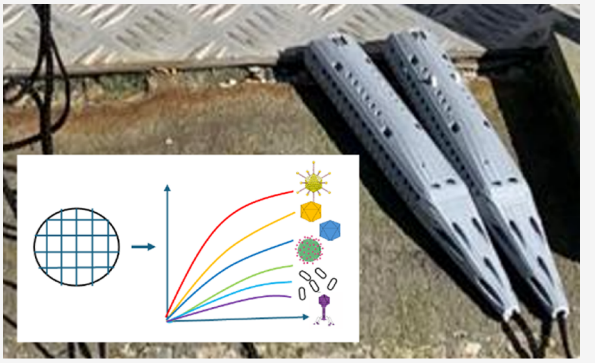

KEYWORDS: *wastewater-based epidemiology, wastewater surveillance, COVID-19, viruses, passive sampling, RT-qPCR, adsorption kinetics*

INTRODUCTION

Wastewater surveillance (WWS) of viral infectious diseases can provide complementary information to clinical and syndromic surveillance.[1] For any wastewater surveillance program, the representativeness of the sampling method is critical. Traditionally, grab or automated composite sampling methods have been utilized. However, grab sampling only yields a snapshot of viral concentrations at a single time point, while composite samplers offer more representative samples but are bulky, costly (∼3000 euros per sampler), and difficult to deploy for in-sewer sampling.[2] In contrast, passive samplers are low cost and rapidly deployable at any scale and provide a time-integrated measure of viral concentrations in wastewater. Given their advantages, passive samplers have become indispensable for targeted surveillance of infectious diseases, such as in upstream locations within wastewater networks such as manholes or lateral house connections. They have been used for monitoring an increasing range of viral pathogens throughout the world.[2−4]

Despite the increasing use of passive samplers, there is little known about the differences in capture kinetics of viruses with varying physio-chemical characteristics. Viruses can exhibit widely different morphologies (filamentous, icosahedral), structures (enveloped or nonenveloped), sizes (15 to over 300 nm hydrodynamic diameter), and isoelectric points (from 3 to over 9).[5] This variability can influence viral behavior at wastewater interfaces, such as partitioning at solid/liquid interfaces.[6,7] Understanding the adsorption behavior of various viruses on passive samplers is critical for the interpretation of results, for example, to reduce the number of false negatives, to choose optimal deployment times, to select normalization methods, or to identify suitable sampling materials for each target virus.[8−10]

Previous work concerning adsorption behavior of viruses on passive samplers has focused on adsorption capacities and kinetics of viruses on electronegative membranes, from

Received: August 14, 2025
Revised: November 24, 2025
Accepted: November 25, 2025
Published: January 23, 2026

https://doi.org/10.1021/acsestwater.5c00976
ACS EST Water 2026, 6, 903−912

wastewater spiked with viral stocks that were produced by cell culture in laboratory conditions, or on-site time-scale experiments for calibration of passive samplers.[8,9,11,12] On-site studies have shown linear uptake of SARS-CoV-2, Pepper Mild Mottle Virus (PMMoV), Enterovirus, and Adenovirus on the electronegative membranes for up to 48 h, while cotton-based passive samplers (tampons/swabs) experienced saturation over 24 h.[8,12] In contrast, studies using heat in-activated SARS-CoV-2 harvested from cell cultures in bench-scale experiments report saturation of membrane and granulated activated carbon (GAC) passive samplers within 24 h.[9,11] However, naturally shed human viruses in wastewater can have different physical properties and attachment behavior compared to viruses harvested from cell cultures, and on-site measurements are difficult to interpret due to the unknown dynamics of wastewater concentrations and physiochemical properties.[9,11] Therefore, the capture kinetics of viruses on passive samplers should also be investigated using naturally shed viruses in bench-scale experiments. Furthermore, so far, there is no study comparing the relative affinities of viruses on passive samplers and the potential biases that are introduced in viral communities by passive sampling. However, understanding capture kinetics of viruses and biases in viral community composition related to sampling methods is critical for representative sampling and correct interpretation of results.

In this study, we aim to determine the uptake rate of naturally shed viruses in wastewater on electronegative membranes. Since exploratory work comparing different passive sampling materials has highlighted higher positivity rates for electronegative membrane passive samplers compared to other commonly used materials (gauze, cotton buds), we focused on electronegative membranes in this study.[2] We performed bench-scale passive sampler incubation experiments to measure the uptake kinetics of different types of viruses. Next, we confirmed differences in the adsorption behavior of target viruses using on-site experiments with passive samplers in a wastewater treatment plant (WWTP). For this study, we focused on two commonly utilized indicator viruses, CrAssphage and PMMoV and four pathogens of public health interest, Human Adenovirus 40/41 (HadV 40/41), Human Norovirus genogroup II (HuNoV GII), Enterovirus, and SARS-CoV-2.

MATERIALS AND METHODS

Wastewater Sampling

To obtain wastewater samples for the batch-incubation experiments, grab sampling of the influent directly after grit screening was performed at a wastewater treatment plant located in the city of Nieuwegein, Netherlands. Nieuwegein WWTP serves approximately 65,971 people (census of 2024) living in the city of Nieuwegein and has a biological design capacity of 159,000 inhabitant equivalents/day and a hydraulic capacity of 3500 m^3/h. It operates at an average capacity of 90.4%. The WWTP receives wastewater from both municipal and industrial sources via a combined sewage system. The influent is on average 1136 m^3/h and displays an average yearly chemical oxygen demand (COD) of 491 mg/L, a pH of 7.8, and a conductivity of 320 μm S/cm.[13]

During the sampling, 2 L polypropylene bottles were filled at 10:30 AM, transported to the laboratory within 30 min, and immediately stored at 4 °C. Wastewater samples were stored for less than 24 h before the incubation experiments were started.

Batch Incubation Experiment Setup

A batch incubation experiment was performed using a wastewater grab sample taken on 11 November 2024. Electronegative membranes (pore size of 0.45 μm, diameter of 47 mm; Cellulose Nitrate Filter, 11406-47-ACN, Sartorius, Germany) were cut in half to ensure free movement in a 250 mL polypropylene tube and incubated in 200 mL of wastewater. An orbital shaker placed inside a 10 °C incubator was set to 150 rpm for agitation. A separate bottle of wastewater, without an electronegative membrane, was included during the incubation period to assess the potential degradation of the viral signal during the experiment.

At time points 1, 3.5, 6.5, 24, and 48 h, three replicate tubes holding electronegative membranes were retrieved from the setup. Membranes were removed from the tubes using sterile tweezers and placed directly inside the lysis buffer (Nucleisens extraction kit, Biomerieux, Amersfoort, The Netherlands), ensuring full submersion. Concurrently, to assess degradation, three 0.5 mL subsamples of wastewater were taken from the tubes without a membrane and placed in lysis buffer. The lysates were vortexed at speed 10 for 30 s using a Vortex Genie 2 (Scientific Industries, Inc., Bohemia, NY, USA). In order to process all samples in a single automated extraction run, lysates were stored at −80 °C for less than 1 week prior to nucleic acid extraction.

Field Deployment Experiments

Field deployment experiments were conducted on two dry weather days (11 November 2024, 06 December 2024) with an outside temperature of 10 ± 5 °C. Electronegative membranes housed in 3D-printed, torpedo style casings[2] were deployed in triplicate for 24 h, where a single membrane was placed inside each of the three torpedo casings. The torpedoes were deployed in the WWTP Nieuwegein influent directly after screening and grit removal. Passive samplers were transported within 30 min to the laboratory and stored at 4 °C until disassembly and preprocessing within 24 h. Grab samples of wastewater were collected during the retrieval of the torpedo samplers to assess the viral concentrations to which the passive samplers were exposed.

Nucleic Acid Extraction and Inhibition Control

Nucleic acid extraction was performed using the semi-automated Nuclisens extraction kit, as described previously.[1] Prior to extraction, wastewater and passive sampler lysates were centrifuged at 4500*g* for 5 min to settle solids that could interfere with the magnetic bead-based extraction process.

An extraction blank was run with each batch, which tested negative for all qPCR targets. Before extraction, approximately 6×10^5 copies of murine hepatitis virus MHV-A59 RNA extract were spiked into all lysates and the extraction blank to test for inhibition and RNA recovery, as described before.[14] The MHV-A59 RNA spike allows assessing recovery throughout the extraction, RT and qPCR steps, and acts as a positive control for the overall process. For all samples, MHV recovery values were comparable and ranged from 19.7% to 40.5%, indicating acceptable recoveries and little to no inhibition (Figure S1).[14]

(RT)-qPCR Assay

Viral concentrations were determined using previously published (RT)-qPCR assays for CrAssphage,[15] PMMoV,[16]

https://doi.org/10.1021/acsestwater.5c00976
ACS EST Water 2026, 6, 903−912

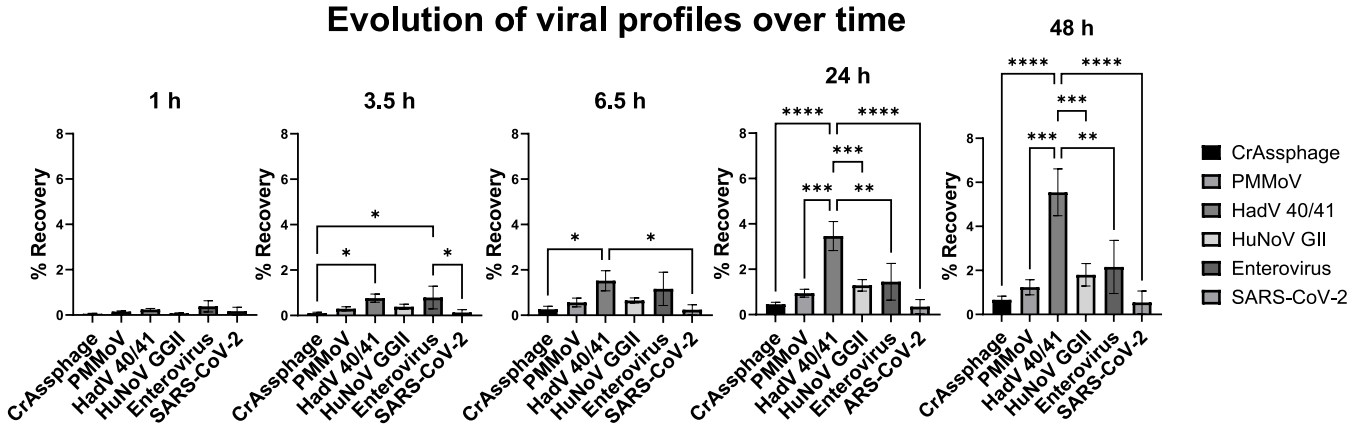

Figure 1. Evolution of viral profiles on the membrane over the 48 h deployment period. The *Y*-axis shows the percentage recovery of viral signal on membranes. The *X*-axis shows the incubation time of passive samplers. Whiskers display the standard deviation of viral concentrations on three membranes ($n = 3$) retrieved from the batch incubation setup at each time point. Pairwise comparisons were performed using ANOVA followed by posthoc Tukey's multiple comparison test ($p < 0.0001$ [****], $p < 0.001$ [***], $p < 0.01$ [**], $p < 0.05$ [*]).

HuNoV GGII,[17] Enterovirus,[18] HadV 40/41,[19] and SARS-CoV-2 N gene.[20] Primers, probes, and reagents used, as well as (RT)-qPCR cycling conditions are reported in Table S1. Each (RT)-qPCR reaction was run in duplicate wells, and mean concentrations were used for further calculations. For each PCR plate, (RT)-qPCR grade water was used as a negative control to assess potential contamination of (RT)-qPCR reagents, which was negative for all plates. (RT)-qPCR assays were performed using the CFX Opus 96 Real-Time PCR System (Bio-Rad Laboratories, Hercules, CA, USA). For quantification of viral loads from Cq values, a standard curve was run on each (RT)-qPCR plate. Standard curves used in quantification and further details on (RT)-qPCR standards used are detailed in the Supporting Information. Standard curve parameters are given in Table S2.

Data Analysis

Viral genome copies per sampler were calculated based on the proportion of lysate used in extraction and proportion of viral extract used in the (RT)-qPCR reaction, as described in SI Section 1.3. Since half membranes were used in batch incubation experiments, the number of viral copies detected on each half membrane was multiplied by two before uptake modeling. Mean concentrations from triplicate tubes analyzed at each time point were used in subsequent uptake and degradation modeling.

Viral Uptake Modeling on Electronegative Membranes and Recovery Rate

Since the initial concentrations varied considerably between viruses, the percent recovery of virus i at each time point was calculated as genetic units (GU) of the viral target on the membrane divided by the total amount of virus i available in the wastewater volume at time 0. Recovery of virus i at time t was calculated as

$$\mathrm{Rec}_{t,i}\left(\frac{\%\ \mathrm{Recovery}}{\mathrm{membrane}}\right) = \frac{N_{t,i,\mathrm{m}}\left(\frac{\mathrm{GU}}{\mathrm{membrane}}\right)}{N_{0,i,\mathrm{ww}}\ (\mathrm{GU})} \times 100$$

where $\mathrm{Rec}_{t,i}$ is the percentage of virus i recovered on the membrane at time t, $N_{t,i,\mathrm{m}}$ is the GU of virus i on the membrane at time t, and $N_{0,i,\mathrm{ww}}$ is the total copies of virus i in incubation wastewater at time 0. Linear and Lagergren's pseudo-first-order (PFO) kinetics were fitted to these percentages of recovered viruses. The linear uptake equation can be described as

$$\mathrm{Rec}_{t,i}\left(\frac{\%\ \mathrm{Recovery}}{\mathrm{membrane}}\right) = \mathrm{RR}_i\left(\frac{\%\ \mathrm{Recovery}}{\mathrm{h} \times \mathrm{membrane}}\right) \times t\ (\mathrm{h}) + \mathrm{Rec}_{0,i}\left(\frac{\%\ \mathrm{Recovery}}{\mathrm{membrane}}\right)$$

$\mathrm{RR_i}$ is the linear recovery rate of virus i on the membrane, and $\mathrm{Rec}_{0,i}$ is the modeled recovery on the membrane at time 0. Recovery at time 0 was not constrained to 0 during fitting due to the initial porewater capacity of membranes, whereby rapid uptake of viruses on the membrane due to porewater uptake during the first minutes of deployment can be expected.

Viral uptake on membranes was also modeled using Lagergren's pseudo-first-order kinetics, which have been widely utilized to model adsorption processes of viruses and chemical contaminants in complex matrices such as wastewater.[9] Pseudo-first-order kinetics (PFO) assume that the uptake rate is proportional to the fraction of available adsorption sites and can be described as

$$\mathrm{Rec}_{t,i}\left(\frac{\%\ \mathrm{Recovery}}{\mathrm{membrane}}\right) = \mathrm{Rec}_{0,i}\left(\frac{\%\ \mathrm{Recovery}}{\mathrm{membrane}}\right) + \left(R_{\mathrm{max},i} - \mathrm{Rec}_{0,i}\left(\frac{\%\ \mathrm{Recovery}}{\mathrm{membrane}}\right)\right)^{1-e^{-K_i \times t}}$$

where $R_{\mathrm{max},i}$ denotes the adsorption capacity of the membrane for virus i, and K_i the pseudo-first-order kinetic constant for the adsorption of virus i on the membrane.

For the PFO kinetic equation, the time to reach half of the modeled adsorption capacity for a given target, commonly referred to as half-time ($t_{1/2}$) was calculated as

$$t_{1/2,i} = \frac{\ln(2)}{K_i}$$

https://doi.org/10.1021/acsestwater.5c00976
ACS EST Water 2026, 6, 903−912

Linear and PFO viral recovery rate modeling was performed using GraphPad Prism 10.4.0. The Shapiro–Wilk test was used to test for normality of residuals ($p > 0.05$ for all models).

Degradation Modeling

Viral degradation during the incubation period was modeled using the first-order degradation model described by the equation below:

$$C_{i,\mathrm{ww}}\left(\frac{\mathrm{GU}}{\mathrm{mL}}\right) = C_{i,0,\mathrm{ww}}\left(\frac{\mathrm{GU}}{\mathrm{mL}}\right) \times \exp(-k_i \times t(h))$$

where $C_{i,\mathrm{ww}}$ is the concentration of virus i in wastewater at time t, $C_{i,0,\mathrm{ww}}$ is the concentration of virus i in wastewater at time = 0, and k_i is the first-order degradation constant for virus i. The first-order degradation model was fit using GraphPad Prism version 10.4.0. To assess if there were statistically significant degradation rates for each virus, a null hypothesis where no degradation occurs ($K_i = 0$) was compared to the first-order degradation model using the extra sum-of-squares F-test.

RESULTS

Evolution of Viral Composition over the Incubation Period

To investigate differences in viral composition on membranes as a function of deployment time, membranes were incubated in wastewater for 2 days and retrieved over a period of 48 h. The percentage recovery of viruses at each time ($\mathrm{Rec}_{t,i}$) was plotted in Figure 1. To determine whether differences in recovery between target viruses were statistically significant, pairwise comparisons were performed using ANOVA followed by posthoc Tukey's multiple comparison test.

For the 24 and 48 h deployment periods, all viruses displayed significantly ($p > 0.001$) lower recovery compared to HadV 40/41, while there were no significant differences in recovery between the other viruses. While selective enrichment of HadV 40/41 was clear during the 24 and 48 h incubation periods, this was not observed in shorter deployment times, demonstrating that viral profiles on the membrane evolve over the deployment time. For instance, during the 3.5 and 6.5 h incubation periods, differences between viral recoveries were only significant ($p > 0.05$) between three pairs (crAssphage/HadV 40/41, crAssphage/Enterovirus, Enterovirus/SARS-CoV-2) and two pairs (crAssphage/HadV 40/41, SARS-CoV-2/HadV 40/41), respectively.

Degradation of Viral Nucleic Acids

While batch-incubation experiments provide a controlled environment to investigate viral uptake, degradation of the viral signal in wastewater could influence the observed uptake rates. Given the lack of data measured in comparable conditions (10 °C, wastewater) and large ranges of viral degradation constants in water matrices reported in the literature,[21,22] we measured the decrease in wastewater viral concentration in incubation wastewater during the 48 h incubation period under identical conditions (150 rpm, 10 °C) using a separate tube of wastewater. Following, these measurements were fit to first-order degradation curves to allow comparison of degradation constants between viruses (Table 2). The concentration measurements and degradation curves are shown in Figure S2. The best-fit first-order degradation constants (10 °C°) for all targets are given in Table 1.

For PMMoV and Enterovirus, no statistically significant degradation was observed over the duration of the incubation experiment ($p < 0.05$, extra-sum of squares F-test), while best-fit first-order-degradation constants ranged from 0.011 h^{-1} to 0.33 h^{-1} for the other targets. The best-fit first-order degradation constant was highest for SARS-CoV-2, followed by HadV 40/41, crAssphage, and HuNoV GII. SARS-CoV-2 exhibited the highest mean degradation constant (0.33 h^{-1}) and over 99% modeled degradation at 48 h.

Table 1. First-Order Degradation Constants $k_{i,10°C}$ (Mean ± Stdev, n = 5, 10 °C, 150 rpm) for Endogenous crAssphage, HadV 40/41, HuNoV GII, and SARS-CoV-2 in Wastewater Samples[a]

	$k_{i,10°C}$ (h^{-1})	Modeled % Degradation at 48 h	R^2
crAssphage	0.016 ± 0.004	53.6	0.88
PMMoV	NS	-	-
HadV 40/41	0.022 ± 0.002	65.2	0.97
HuNoV GII	0.011 ± 0.002	41.0	0.91
Enterovirus	NS	-	-
SARS-CoV-2	0.33 ± 0.12	99.99	0.85

[a]Modeled degradation based on best-fit first-order degradation rates are reported.

On-Site Viral Uptake

Viral uptake in bench-scale experiments may differ from field conditions, such as in the flow and concentration dynamics of viruses.[23] To investigate if differences in virus recovery between the different targets are also observed under field conditions, two separate days of 24 h field deployment experiments using 3D-printed torpedo passive samplers loaded with electronegative membrane filters were performed.[2] Since the exact virus dynamics in bulk wastewater to which passive samplers are exposed are unknown, we calculated relative capture as the wastewater mL equivalent of the viral load from the wastewater that was used for the capture study.[8]

Upon 24 h deployment, a significantly higher mL equivalent of HadV 40/41 compared to crAssphage, PMMoV, HuNoV GII, Enterovirus, and SARS-CoV-2 was detected on Day 1 (11/11/24). The differences observed on Day 2 (06/12/24) were not statistically significant (Figure 2). On both days, the mean mL equivalent of HadV 40/41 captured was higher than other targets, supporting our observations during lab-scale incubation experiments.

Uptake Modeling of Viruses on Electronegative Membranes

To better understand differences in the uptake of naturally shed viruses on electronegative membrane passive samplers, we modeled uptake rates for all target viruses using Linear/PFO kinetics. We chose to use linear and PFO uptake kinetic models due to their previous use in modeling viral uptake kinetics in wastewater on passive samplers.[8,9,11] Absolute uptake rates of viruses on membranes were modeled first (Table S2 and Figure S3). However, uptake rates were influenced by large initial differences in virus concentrations in wastewater (Figure 3).

Since absolute uptake rates did not represent an adequate comparison between viruses, percent recovery (Figure 1) rather than absolute numbers was calculated to describe virus-passive interactions. Both linear and PFO kinetics were used to investigate viral recovery rates. Linear and PFO model curves are displayed in Figure 4. For both models, adjusted R^2 values ranged between 0.85 and 0.99 and the standard deviation of residuals (Sy.x) ranged between 0.036 and 0.37 (Table 2).

https://doi.org/10.1021/acsestwater.5c00976
ACS EST Water 2026, 6, 903–912

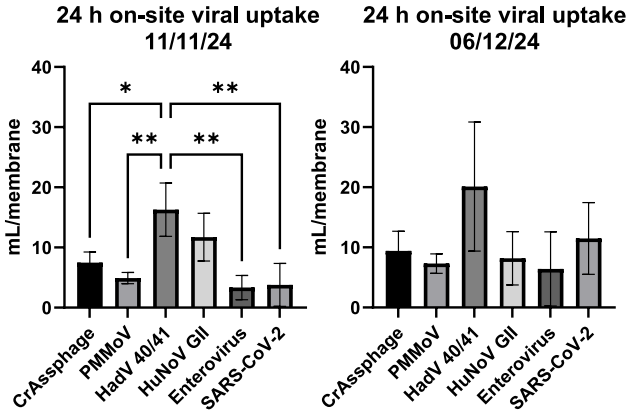

Figure 2. Wastewater viral capture (24 h, 10 ± 5 °C) at Nieuwegein WWTP influent on two different days (left: 11 November 24, right: 06 December 24) of on-site deployment. *X*-axis: Virus type. *Y*-axis: crAssphage, PMMoV, HadV 40/41, HuNoV GII, Enterovirus copies captured normalized by bulk wastewater concentrations. Whiskers display the standard deviation of viral concentrations measured from three torpedoes (n = 3) deployed on each date. Pairwise comparisons were performed using ANOVA followed by posthoc Tukey's multiple comparison test (p < 0.01 [**], p < 0.05 [*]).

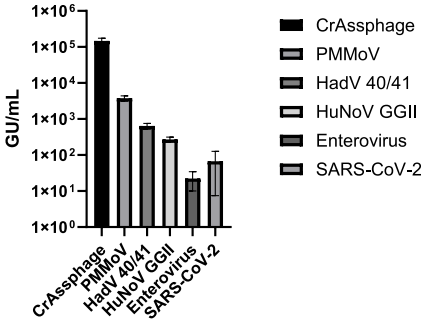

Figure 3. Initial wastewater viral concentrations in gene units per mL for CrAssphage, PMMoV, HadV 40/41, Enterovirus, and SARS-CoV-2 vary by orders of magnitude. *X*-axis: Target virus. *Y*-axis: Wastewater concentration of viruses measured at t = 0 displayed in log10 scale. Whiskers display the standard deviation of viral concentrations measured at the start of the incubation period (n = 3).

During the 48 h experiments, none of the viral targets reached saturation on the membrane surface (Figure 4). For the target viruses, the $t_{1/2}$ value was highest for SARS-CoV-2, followed by HadV 40/41, Enterovirus, CrAssphage, HuNoV GII, and PMMoV. The modeled adsorption capacity ($R_{max,i}$) for HadV 40/41 was highest, followed by Enterovirus, HuNoV GII, SARS-CoV-2, PMMoV, and CrAssphage. However, it is critical to note that since saturation was not reached in the given experiment, modeled adsorption capacities, as the outcome of the PFO equation (Table 2) should be treated with caution.

DISCUSSION

Evolution of Viral Uptake on Electronegative Membranes during Deployment

Viral recoveries on the electronegative membrane surface were significantly (p < 0.001) different for HadV 40/41 to all other virus targets for 24 and 48 h deployments, while these differences were less clear for 3.5 and 6.5 h deployments. Based on our observations, it is apparent that longer deployment periods gradually result in the selective enrichment of HadV 40/41. This observation is supported by results from Li et al. 2022, where the on-site viral uptake kinetics on electronegative membranes was investigated. Results from this study report a higher wastewater volume equivalent uptake of HadV 40/41 (33.1 mL/h) compared to Enterovirus (0.3 mL/h) and PMMoV (1 mL/h), respectively.[8] Furthermore, exploratory studies using target-enrichment sequencing with electronegative membrane sampling also indicate selective enrichment of Mastadenoviruses (including HadV 40/41) on membranes but not for composite samples.[24]

Despite the selective enrichment of HadV 40/41 on electronegative membranes, no significant differences were observed in the recovery of CrAssphage, PMMoV, HuNoV GII, Enterovirus, and SARS-CoV-2. Previous research has highlighted that the differential binding kinetics of targets can hinder the use of markers such as PMMoV and CrAssphage for normalization in passive sampling.[10,25,26] Based on our recovery experiments, both markers are suitable, yielding results comparable to those of direct wastewater samples. However, it is important to note that uptake kinetics at close-to-source locations with greater concentration variations may differ.

The observed biases have important implications for the choice of deployment times and sampling methods. For example, the increased sensitivity for monitoring HadV 40/41 with electronegative membranes or the potential for a skewed view of the wastewater virome in metagenomics studies. Further work to identify these biases will help guide the use of passive sampling materials, with the prospect of improving sensitivity for viral monitoring and clarifying the inherent limitations and advantages of different sampling methods.

Degradation of Viral Nucleic Acids

In the incubation experiments, differences between degradation rates between viruses could affect the observed recoveries. Therefore, to assess whether biases observed in viral recoveries on membranes were affected by degradation, we measured degradation rates for all viral targets in a parallel experiment. In general, degradation rates of viruses measured in water environments are difficult to compare due to highly variable results reported in the literature.[21,22] This variations in measurements can be attributed to a variety of factors, including but not limited to differences in wastewater physiochemical characteristics, differences in regions targeted for quantification by (RT)-qPCR, exposure to sunlight, quantification methods (e.g., culture, (RT)-qPCR), or differences in spiked viruses and viruses naturally shed into wastewater.[21,22,27,28] Nonetheless, our measurements roughly agree with the literature, where mean first-order degradation constants in a meta-analysis of 562 articles measuring degradation rates for mammalian viruses and coliphages noted that mean degradation rates (in experiments performed at 4 °C−29 °C) range between 0.0029 and 0.038 h^{-1}. In contrast to mammalian viruses, PMMoV, a plant virus with a significantly different structure, has been observed to be very stable in wastewater (4−20 °C) with mean first-order degradation constants ranging from 0.0005 to 0.0064 h^{-1}, confirming our results where no significant degradation of PMMoV through the 2-day period was observed.[29]

An inherent limitation of this study is the low number of copies of naturally shed enteroviruses and SARS-CoV-2 during the sampling period, which resulted in high variability between

https://doi.org/10.1021/acsestwater.5c00976
ACS EST Water 2026, 6, 903−912

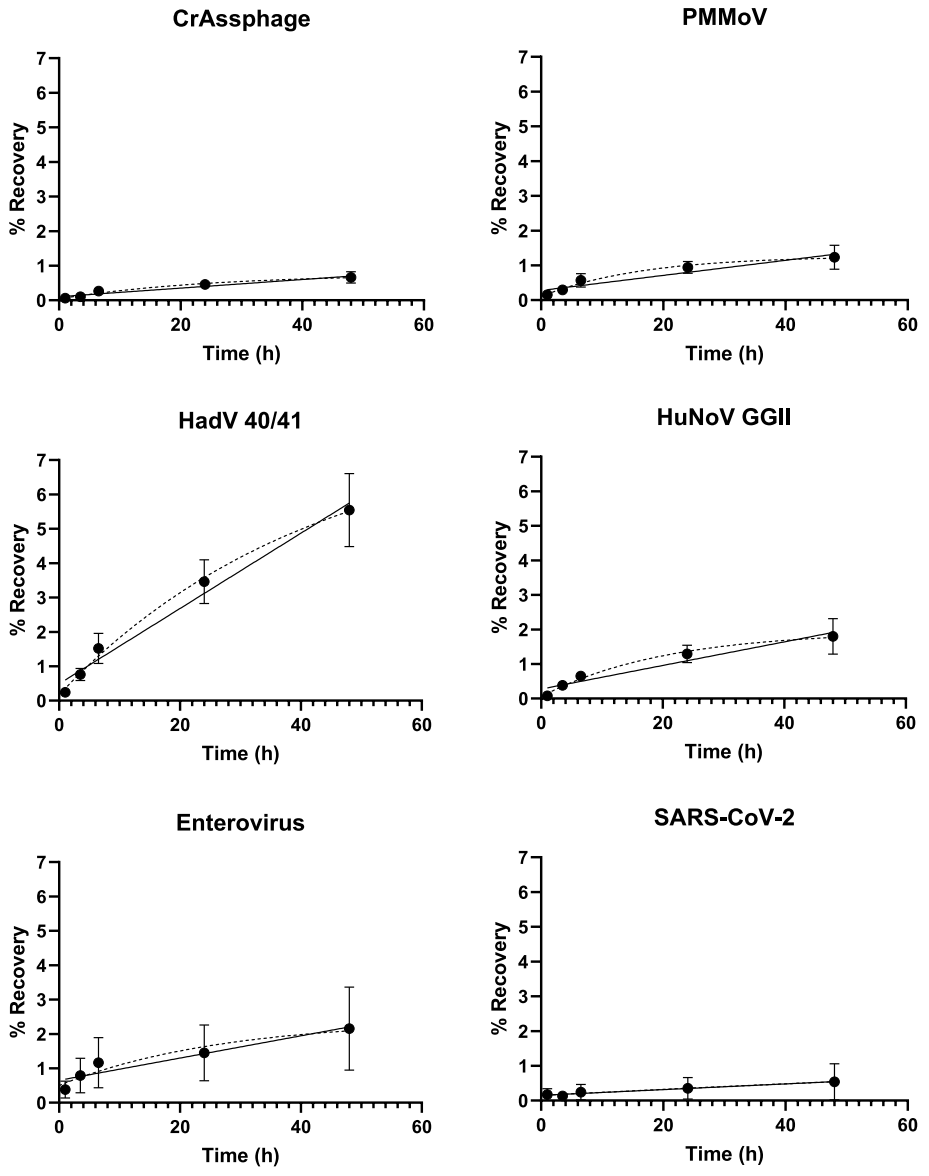

Figure 4. Mean percent viral recovery on membrane passive samplers (circles) during 10 °C incubation experiments was fitted with linear (solid line) and PFO (dashed line) kinetic models. Error bars display the standard deviation of viral concentrations measured (n = 3) at each time point. Error bars are not visible when smaller than symbols.

Table 2. Best-Fit Values for Linear and PFO Kinetic Model Parameters (T = 10 °C, n = 5) for Each Virus and Goodness-of-Fit for the Models (Adjusted R^2 and Sy.x)[a]

	Linear Uptake Model				PFO Model					
	RR_i (fraction GU/h/membrane)	$Rec_{0,i}$ (fraction GU/membrane)	Adjusted R^2	Sy.x	K_i (1/h)	$t_{1/2}$ (h)	$R_{max,i}$ (fraction GU/membrane)	$Rec_{0,i}$ (fraction GU/membrane)	Adjusted R^2	Sy.x
crAssphage	0.012	0.10	0.92	0.072	0.040	17.2	0.76	0.04	0.96	0.051
PMMoV	0.022	0.28	0.88	0.16	0.061	11.4	1.27	0.10	0.97	0.077
HadV 40/41	0.11	0.49	0.97	0.37	0.024	29.3	8.03	0.17	0.99	0.20
HuNoV GII	0.034	0.27	0.91	0.21	0.049	14.2	1.95	0.057	0.98	0.096
Enterovirus	0.032	0.65	0.86	0.25	0.037	18.6	2.41	0.50	0.85	0.26
SARS-CoV-2	0.0082	0.15	0.95	0.036	0.0052	133.4	1.94	0.15	0.93	0.043

[a]For linear recovery rates, two parameters, RR_i, linear recovery rate, $Rec_{0,i}$ modeled recovery fraction on membrane at T = 0 describe the model. For the PFO model, K_i PFO recovery constant, $t_{1/2}$: half-time, $R_{max,i}$ modeled maximum recovery fraction, $Rec_{0,i}$ modeled recovery fraction on membrane at T = 0.

replicates for these two targets and made it difficult to accurately determine their degradation rates. However, SARS-CoV-2 was the only enveloped virus analyzed in this study and displays a higher degradation rate than the other viral targets, consistent with previous observations that enveloped viruses generally degrade more rapidly than nonenveloped viruses.[22]

https://doi.org/10.1021/acsestwater.5c00976
ACS EST Water 2026, 6, 903−912

Degradation of viral signal can result in lower observed uptake rates because of the decreased availability of viruses in bulk wastewater, as well as degradation of viral nucleic acids already captured on the membrane surface. For CrAssphage, HadV 40/41, HuNoV GII, and SARS-CoV-2% of modeled viral degradation in bulk wastewater during the 48 h experiments were 53%, 65%, 41%, and 99%, respectively (Table 1). It is difficult to quantitatively assess the impact of degradation on our results due to potential differences between viral degradation in bulk wastewater and that on the membrane surface. Previous studies have shown that stabilization on a surface can enhance the survivability of viruses, for example, it has been suggested that viral nucleic acids could be stabilized by partitioning to wastewater solids[30] or sediments.[31] However, given the comparable degradation rates observed for CrAssphage, HadV 40/41, and HuNoV GII, the higher enrichment of HadV 40/41 is more likely attributable to a higher affinity for the membrane rather than to higher stability.

Observations on viral degradation rates are difficult to translate quantitatively to on-site conditions, where both capture and degradation of viruses on passive samplers can be expected to vary depending on the concentration dynamics. For instance, if viral uptake on the passive samplers was due to a large concentration spike at the start of the deployment period, the viral signal detected will be affected by degradation more significantly than if the uptake happened at a later period, where virus particles retrieved on the passive sampler will have less time to degrade. In an on-site deployment scenario, the passive samplers are not affected by degradation in bulk wastewater in the same way as batch incubation experiments, where a fresh "batch" of virus could pass by the sampler at any time point during the deployment. Therefore, considering the complexity of capture and degradation dynamics on passive samplers, viral composition on passive samplers deployed on-site can be determined not only by virus-passive biases but also by a complex combination of wastewater concentration dynamics and degradation.

On-Site Viral Uptake Biases

While batch experiments performed under laboratory conditions can provide a controlled environment to study viral uptake on passive samplers, they are only partially representative of on-site conditions. Given the discussed complexities, we performed on-site 24 h deployment experiments and observed similar trends in on-site and bench-scale experiments, where a higher mean HadV 40/41 capture compared to all targets was detected on both deployment days. Triplicate measurements on-site had a higher variation between measurements, and differences between viral capture were not consistently significant. It has been hypothesized that this increase in variation could result from differences in flow conditions inside torpedo passive samplers.[32] Nevertheless, similar trends between on-site experiments and the batch incubation experiments, as well as on-site deployments by Li et al. 2022 and target enrichment sequencing results support the selective enrichment of HadV 40/41.

However, as discussed also in previous sections, while viral concentrations are only affected by degradation and uptake of viruses in batch experiments, on-site conditions are dynamic, where concentrations of viruses, wastewater characteristics, as well as flow conditions can vary throughout the day. Especially in upstream locations, where passive samplers are typically preferred due to the lack of automated sampling infrastructure, wastewater dynamics can have a more significant effect on captured viral compositions than WWTP influents. Further work should aim to determine if the differences between viral uptake on electronegative membranes can also be observed in upstream locations, where more significant variations in concentration and flow conditions can be expected.

Uptake Modeling of Viruses on Electronegative Membranes

This study showed that electronegative membranes experience minimal saturation for up to 48 h of deployment. Linear and PFO kinetic equations have been previously used to describe the uptake of viruses on electronegative membranes.[8,9,11] In the PFO model, the uptake rate is governed by the fraction of available sites on the passive sampler surface, while for the linear model, the uptake rate is constant throughout the incubation period. Compared to the PFO model, the linear model can provide an adequate description of viral uptake on surfaces if saturation of the adsorption surface during the deployment period is minimal, for example, if the uptake of viruses during deployment compared to the available sites is low.

Comparing the two models, for all of the viral targets except Enterovirus and SARS-CoV-2, adjusted R^2 values were higher and Sy.x was lower for the PFO model, indicating that the PFO model better described the uptake on membranes for the majority of target viruses. For Enterovirus and SARS-CoV-2, the uptake was better described by the linear model, suggesting that saturation on the membrane surface for these viruses was minimal throughout the 48 h deployment period. However, it is important to note that given the very low concentrations of these viruses in wastewater, the variability between replicates was high. Therefore, we expect that the modeled uptake/recovery rates are more accurate for viruses found in higher concentrations. Despite limitations due to variable concentrations of naturally shed viruses, the PFO model parameters make clear that relative adsorption capacities and saturation times vary for different viruses. In the PFO model, half-time ($t_{1/2}$) values can describe how fast the system reaches equilibrium, while $R\max_i$ describes the adsorption capacity of the membrane for a given virus. For SARS-CoV-2 and HadV 40/41, $t_{1/2}$ values were above 48 h, signifying limited saturation (less than half of the modeled adsorption capacity) over the deployment period, while faster saturation was observed for the other targets. On the other hand, best-fit adsorption capacity was highest for HadV 40/41, followed by Enterovirus, HuNoV GII, SARS-CoV-2, PMMoV, and CrAssphage. Given the differences in adsorption characteristics, we observe that viral uptake capacities and appropriate deployment times for capture of viruses on electronegative membranes are dependent on the target virus.

In comparison to our results, there are few studies focusing on modeling the uptake kinetics of viruses on passive samplers and only two explicitly modeled viral uptake on electronegative membrane passive samplers.[8,9,11,12] The first study, Hayes et al. 2022, modeled the uptake rate of lab-grown viruses[9] spiked in wastewater on electronegative membranes, while the second study, Li et al. 2022, modeled uptake based on data from on-site passive sampling of naturally shed viruses in wastewater. Interestingly, while Hayes et al. 2022 observed saturation of membranes within 24 h, Li et al. 2022 reported linear uptake of naturally shed viruses in wastewater on the membrane surface for up to 48 h. We observed pseudo-first-order/linear uptake of

https://doi.org/10.1021/acsestwater.5c00976
ACS EST Water 2026, 6, 903−912

naturally shed viruses on electronegative membranes with no saturation within the 48 h period. We therefore hypothesize that the contrasting results between Hayes et al. 2022 and Li et al. 2022 and our study can be attributed to inherent differences between naturally shed and lab-grown viruses. Supporting our observations, a recent study spiking naturally shed viruses in wastewater into groundwater samples has also observed increasing viral loads up to 72 h for HadV 40/41 and PMMoV uptake on electronegative membrane passive samplers.[32] In contrast to naturally shed viruses, viruses harvested from cell culture in the laboratory and spiked into wastewater can exhibit significantly different physicochemical characteristics such as isoelectric point and hydrophobicity or morphologies,[5] which can affect uptake behavior on passive samplers.

Given the recovery rates, it is clear that longer deployment times (over 48 h) are required to reach the adsorption capacity of membrane passive samplers. While the majority of previous studies using passive samplers have used 24 h or shorter deployment periods, we observe that longer time-integrated sampling periods are feasible for the viruses in this study.[2,12,24] However, it is important to note that on-site dynamics of viral concentrations and flow conditions can be critical in uptake, especially in upstream locations, such as manholes, where passive samplers are often used for viral monitoring. Depending on the size of the catchment and target virus, the concentration dynamics of viruses can vary significantly. For viruses shed by a majority of the population such as CrAssphage and PMMoV, diurnal variations at large wastewater catchments such as WWTP influents have been observed to be low.[33,34] However, for pathogenic viruses with low incidence rates, concentration variations through the deployment period can be highly variable, where uptake of viruses is likely dependent on the ability of passive samplers to capture shorter spikes in viral concentrations. Moreover, there is little known about the ability of passive samplers to retain the captured viral material during periods of low viral concentrations. For example, dilution of wastewater flow by rainfall might result in low concentration periods and potential washoff of captured signals from passive samplers.[12,23] Due to the aforementioned limitations, our observations more accurately represent the capture of viruses in larger catchment sizes such as pumping stations or wastewater treatment plants, where wastewater characteristics and concentration dynamics are more stable. Therefore, we expect that longer deployment periods could be advantageous for the sensitivity of viral monitoring using passive samplers, given that catchment sizes targeted are large enough to minimize large spikes in viral concentrations. However, further research on the ability of passives to capture spikes in viral concentrations as well as the reversibility of viral capture on passives is required to better understand viral uptake at small catchment sizes such as individual buildings or manholes.

CONCLUSION

This work investigated the uptake kinetics of naturally shed CrAssphage, PMMoV, Human Adenovirus 40/41, Norovirus GGII, and Enterovirus in wastewater on electronegative membranes using bench-scale/on-site experiments. We observed that linear/PFO uptake models both adequately described (adjusted R^2: 0.89−0.99 for both models) 48 h uptake of the target viruses, where viral profiles evolved over the deployment period with enrichment of HadV 40/41, while no differences in recovery between other viruses were observed. Based on our results, we recommend that potential biases in viral composition introduced by different deployment times or passive sampler−virus interactions are taken into account during the choice of sampling and normalization methods. These differences are critical in the interpretation of results and choice of appropriate sampling methodology and can result in increased/decreased sensitivity for monitoring different kinds of viruses using passive samplers. To increase the applicability of passive sampling for WWS, further research should aim to elucidate differences between various passive sampling materials (e.g., cotton-based materials, granulated activated carbon) in capturing viruses of varying physiochemical characteristics.

ASSOCIATED CONTENT

Supporting Information

The Supporting Information is available free of charge at https://pubs.acs.org/doi/10.1021/acsestwater.5c00976.

MHV recovery, additional details on viral concentration calculations, and absolute uptake rate modeling (PDF)

AUTHOR INFORMATION

Corresponding Author

Adnan Ege Sener − *TU Delft, Department of Water Management, Delft 2628 CN, The Netherlands; KWR Water Research Institute, Nieuwegein 3433 PE, The Netherlands;* orcid.org/0009-0006-1952-2767; Email: ege.sener@kwrwater.nl

Authors

Leo Heijnen − *KWR Water Research Institute, Nieuwegein 3433 PE, The Netherlands*

Miranda de Graaf − *Erasmus MC, Department of Viroscience, Rotterdam 3015 GD, The Netherlands*

Jeroen Langeveld − *TU Delft, Department of Water Management, Delft 2628 CN, The Netherlands; Partners4UrbanWater, Nijmegen 6532 ZV, The Netherlands*

Gertjan Medema − *TU Delft, Department of Water Management, Delft 2628 CN, The Netherlands; KWR Water Research Institute, Nieuwegein 3433 PE, The Netherlands;* orcid.org/0000-0003-0475-6465

Complete contact information is available at: https://pubs.acs.org/10.1021/acsestwater.5c00976

Funding

This project was supported by funding from the Pandemic Disaster Preparedness Center under the frontrunner project INSPECT.

Notes

The authors declare no competing financial interest.

ACKNOWLEDGMENTS

We thank Ben Vis and all RZWI-Nieuwegein staff for their technical assistance during wastewater sampling.

REFERENCES

(1) Medema, G.; Heijnen, L.; Elsinga, G.; Italiaander, R.; Brouwer, A. Presence of SARS-Coronavirus-2 RNA in Sewage and Correlation with Reported COVID-19 Prevalence in the Early Stage of the

Epidemic in The Netherlands. *Environ. Sci. Technol. Lett.* **2020**, *7* (7), 511−516.
(2) Schang, C.; Crosbie, N. D.; Nolan, M.; Poon, R.; Wang, M.; Jex, A.; John, N.; Baker, L.; Scales, P.; Schmidt, J.; Thorley, B. R.; Hill, K.; Zamyadi, A.; Tseng, C.-W.; Henry, R.; Kolotelo, P.; Langeveld, J.; Schilperoort, R.; Shi, B.; Einsiedel, S.; Thomas, M.; Black, J.; Wilson, S.; McCarthy, D. T. Passive Sampling of SARS-CoV-2 for Wastewater Surveillance. *Environ. Sci. Technol.* **2021**, *55* (15), 10432−10441.
(3) Bivins, A.; Kaya, D.; Ahmed, W.; Brown, J.; Butler, C.; Greaves, J.; Leal, R.; Maas, K.; Rao, G.; Sherchan, S.; Sills, D.; Sinclair, R.; Wheeler, R. T.; Mansfeldt, C. Passive Sampling to Scale Wastewater Surveillance of Infectious Disease: Lessons Learned from COVID-19. *Sci. Total Environ.* **2022**, *835*, 155347.
(4) N, E. K.; Law, I.; Weese, J. S.; McCarthy, D. T.; Murphy, H. Passive Sampling of Microbes in Various Water Sources: A Systematic Review. *Water Res.* **2024**, *266*, 122284.
(5) David, M. K.; Howley, P. *Field Virology*, 6 th ed.; Lippincott Williams & Wilkins (LWW), 2013.
(6) Armanious, A.; Aeppli, M.; Jacak, R.; Refardt, D.; Sigstam, T.; Kohn, T.; Sander, M. Viruses at Solid−Water Interfaces: A Systematic Assessment of Interactions Driving Adsorption. *Environ. Sci. Technol.* **2016**, *50* (2), 732−743.
(7) Schijven, J. F.; Hassanizadeh, S. M. Removal of Viruses by Soil Passage: Overview of Modeling, Processes, and Parameters. *Crit. Rev. Environ. Sci. Technol.* **2000**, *30* (1), 49−127.
(8) Li, J.; Verhagen, R.; Ahmed, W.; Metcalfe, S.; Thai, P. K.; Kaserzon, S. L.; Smith, W. J. M.; Schang, C.; Simpson, S. L.; Thomas, K. V.; Mueller, J. F.; Mccarthy, D. In Situ Calibration of Passive Samplers for Viruses in Wastewater. *ACS EST Water* **2022**, *2* (11), 1881−1890.
(9) Hayes, E. K.; Sweeney, C. L.; Fuller, M.; Erjavec, G. B.; Stoddart, A. K.; Gagnon, G. A. Operational Constraints of Detecting SARS-CoV-2 on Passive Samplers Using Electronegative Filters: A Kinetic and Equilibrium Analysis. *ACS EST Water* **2022**, *2*, 1910−1920.
(10) Langeveld, J.; Schilperoort, R.; Heijnen, L.; Elsinga, G.; Schapendonk, C. E. M.; Fanoy, E.; De Schepper, E. I. T.; Koopmans, M. P. G.; De Graaf, M.; Medema, G. Normalisation of SARS-CoV-2 Concentrations in Wastewater: The Use of Flow, Electrical Conductivity and crAssphage. *Sci. Total Environ.* **2023**, *865*, 161196.
(11) Hayes, E. K.; Stoddart, A. K.; Gagnon, G. A. Adsorption of SARS-CoV-2 onto Granular Activated Carbon (GAC) in Wastewater: Implications for Improvements in Passive Sampling. *Sci. Total Environ.* **2022**, *847*, 157548.
(12) Habtewold, J.; McCarthy, D.; McBean, E.; Law, I.; Goodridge, L.; Habash, M.; Murphy, H. M. Passive Sampling, a Practical Method for Wastewater-Based Surveillance of SARS-CoV-2. *Environ. Res.* **2022**, *204*, 112058.
(13) Van Den Brand, T. P. H.; Roest, K.; Chen, G. H.; Brdjanovic, D.; Van Loosdrecht, M. C. M. Occurrence and Activity of Sulphate Reducing Bacteria in Aerobic Activated Sludge Systems. *World J. Microbiol. Biotechnol.* **2015**, *31* (3), 507−516.
(14) Heijnen, L.; Elsinga, G.; De Graaf, M.; Molenkamp, R.; Koopmans, M. P. G.; Medema, G. Droplet Digital RT-PCR to Detect SARS-CoV-2 Signature Mutations of Variants of Concern in Wastewater. *Sci. Total Environ.* **2021**, *799*, 149456.
(15) Stachler, E.; Kelty, C.; Sivaganesan, M.; Li, X.; Bibby, K.; Shanks, O. C. Quantitative CrAssphage PCR Assays for Human Fecal Pollution Measurement. *Environ. Sci. Technol.* **2017**, *51* (16), 9146−9154.
(16) Haramoto, E.; Kitajima, M.; Kishida, N.; Konno, Y.; Katayama, H.; Asami, M.; Akiba, M. Occurrence of Pepper Mild Mottle Virus in Drinking Water Sources in Japan. *Appl. Environ. Microbiol.* **2013**, *79* (23), 7413−7418.
(17) Kageyama, T.; Kojima, S.; Shinohara, M.; Uchida, K.; Fukushi, S.; Hoshino, F. B.; Takeda, N.; Katayama, K. Broadly Reactive and Highly Sensitive Assay for Norwalk-Like Viruses Based on Real-Time Quantitative Reverse Transcription-PCR. *J. Clin. Microbiol.* **2003**, *41* (4), 1548−1557.
(18) Lodder, W. J.; Wuite, M.; De Roda Husman, A. M.; Rutjes, S. A. Environmental Surveillance of Human Parechoviruses in Sewage in the Netherlands. *Appl. Environ. Microbiol.* **2013**, *79* (20), 6423−6428.
(19) Jothikumar, N.; Cromeans, T. L.; Hill, V. R.; Lu, X.; Sobsey, M. D.; Erdman, D. D. Quantitative Real-Time PCR Assays for Detection of Human Adenoviruses and Identification of Serotypes 40 and 41. *Appl. Environ. Microbiol.* **2005**, *71* (6), 3131−3136.
(20) Lu, X.; Wang, L.; Sakthivel, S. K.; Whitaker, B.; Murray, J.; Kamili, S.; Lynch, B.; Malapati, L.; Burke, S. A.; Harcourt, J.; Tamin, A.; Thornburg, N. J.; Villanueva, J. M.; Lindstrom, S. US CDC Real-Time Reverse Transcription PCR Panel for Detection of Severe Acute Respiratory Syndrome Coronavirus 2. *Emerg. Infect. Dis.* **2020**, *26* (8), 1654−1665.
(21) Boehm, A. B.; Silverman, A. I.; Schriewer, A.; Goodwin, K. Systematic Review and Meta-Analysis of Decay Rates of Waterborne Mammalian Viruses and Coliphages in Surface Waters. *Water Res.* **2019**, *164*, 114898.
(22) Silverman, A. I.; Boehm, A. B. Systematic Review and Meta-Analysis of the Persistence of Enveloped Viruses in Environmental Waters and Wastewater in the Absence of Disinfectants. *Environ. Sci. Technol.* **2021**, *55* (21), 14480−14493.
(23) Jones, D. L.; Grimsley, J. M. S.; Kevill, J. L.; Williams, R.; Pellett, C.; Lambert-Slosarska, K.; Singer, A. C.; Williams, G. B.; Bargiela, R.; Brown, R. W.; Wade, M. J.; Farkas, K. Critical Evaluation of Different Passive Sampler Materials and Approaches for the Recovery of SARS-CoV-2, Faecal-Indicator Viruses and Bacteria from Wastewater. *Water* **2022**, *14* (21), 3568.
(24) Mejías-Molina, C.; Pico-Tomàs, A.; Beltran-Rubinat, A.; Martínez-Puchol, S.; Corominas, L.; Rusiñol, M.; Bofill-Mas, S. Effectiveness of Passive Sampling for the Detection and Genetic Characterization of Human Viruses in Wastewater. *Environ. Sci. Water Res. Technol.* **2023**, *9* (4), 1195−1204.
(25) de Jong, M.; van der Loeff, M. F. S.; Schilperoort, R.; Vennema, H.; van der Weijden, C.; Langeveld, J.; Welkers, M.; Prins, M.; Husman, A. M. R.; Fanoy, E.; et al. Use of passive samplers as sewage surveillance tool to monitor a hepatitis A outbreak at a school in Amsterdam, the Netherlands, Oct 2022 − March 2023. *BMC Infect. Dis.* **2024**, *24*, 1044.
(26) Farkas, K.; Kevill, J. L.; Adwan, L.; Garcia-Delgado, A.; Dzay, R.; Grimsley, J. M. S.; Lambert-Slosarska, K.; Wade, M. J.; Williams, R. C.; Martin, J.; Drakesmith, M.; Song, J.; McClure, V.; Jones, D. L. Near-Source Passive Sampling for Monitoring Viral Outbreaks within a University Residential Setting. *Epidemiol. Infect.* **2024**, *152*, No. e31.
(27) Kennedy, L. C.; Costantini, V. P.; Huynh, K. A.; Loeb, S. K.; Jennings, W. C.; Lowry, S.; Mattioli, M. C.; Vinjé, J.; Boehm, A. B. Persistence of Human Norovirus (GII) in Surface Water: Decay Rate Constants and Inactivation Mechanisms. *Environ. Sci. Technol.* **2023**, *57* (9), 3671−3679.
(28) Mercier, É.; D'Aoust, P. M.; Eid, W.; Hegazy, N.; Kabir, P.; Wan, S.; Pisharody, L.; Renouf, E.; Stephenson, S.; Graber, T. E.; MacKenzie, A. E.; Delatolla, R. Sewer Transport Conditions and Their Role in the Decay of Endogenous SARS-CoV-2 and Pepper Mild Mottle Virus from Source to Collection. *Int. J. Hyg. Environ. Health* **2025**, *263*, 114477.
(29) Burnet, J.-B.; Cauchie, H.-M.; Walczak, C.; Goeders, N.; Ogorzaly, L. Persistence of Endogenous RNA Biomarkers of SARS-CoV-2 and PMMoV in Raw Wastewater: Impact of Temperature and Implications for Wastewater-Based Epidemiology. *Sci. Total Environ.* **2023**, *857*, 159401.
(30) Roldan-Hernandez, L.; Graham, K. E.; Duong, D.; Boehm, A. B. Persistence of Endogenous SARS-CoV-2 and Pepper Mild Mottle Virus RNA in Wastewater-Settled Solids. *ACS EST Water* **2022**, *2* (11), 1944−1952.
(31) Ahmed, W.; Zhang, Q.; Kozak, S.; Beale, D.; Gyawali, P.; Sadowsky, M. J.; Simpson, S. Comparative Decay of Sewage-Associated Marker Genes in Beach Water and Sediment in a Subtropical Region. *Water Res.* **2019**, *149*, 511−521.
(32) Mejías-Molina, C.; Estarlich-Landajo, I.; Martínez-Puchol, S.; Bofill-Mas, S.; Rusiñol, M. Exploring Waterborne Viruses in

Groundwater: Quantification and Virome Characterization via Passive Sampling and Targeted Enrichment Sequencing. *Water Res.* **2024**, *266*, 122305.
(33) Farkas, K.; Pântea, I.; Woodhall, N.; Williams, D.; Lambert-Slosarska, K.; Williams, R. C.; Grimsley, J. M. S.; Singer, A. C.; Jones, D. L. Diurnal Changes in Pathogenic and Indicator Virus Concentrations in Wastewater. *Environ. Sci. Pollut. Res.* **2023**, *30* (59), 123785−123795.
(34) Ahmed, W.; Bivins, A.; Bertsch, P. M.; Bibby, K.; Gyawali, P.; Sherchan, S. P.; Simpson, S. L.; Thomas, K. V.; Verhagen, R.; Kitajima, M.; Mueller, J. F.; Korajkic, A. Intraday Variability of Indicator and Pathogenic Viruses in 1-h and 24-h Composite Wastewater Samples: Implications for Wastewater-Based Epidemiology. *Environ. Res.* **2021**, *193*, 110531.

https://doi.org/10.1021/acsestwater.5c00976
ACS EST Water 2026, 6, 903−912